Electronic Supplementary Material (ESI) for Physical Chemistry Chemical Physics.

Kinetic Studies of C_1 and C_2 Criegee Intermediates with SO_2 using Laser Flash Photolysis coupled with Photoionization Mass Spectrometry and Time Resolved UV Absorption Spectrometry

N.U.M Howes, Z.S. Mir, M.A. Blitz* S. Hardman, T.R. Lewis, D. Stone and P.W. Seakins*

School of Chemistry, University of Leeds, Leeds, LS2 9JT, UK

Supplementary Information

Contents

1. Simulations of CH_2OO decays to determine the relative contribution of first and second order kinetics

Scheme S1 shows possible reactions of the CH_2OO Criegee intermediate following generation by flash photolysis of CH_2I_2 in the presence of excess oxygen.

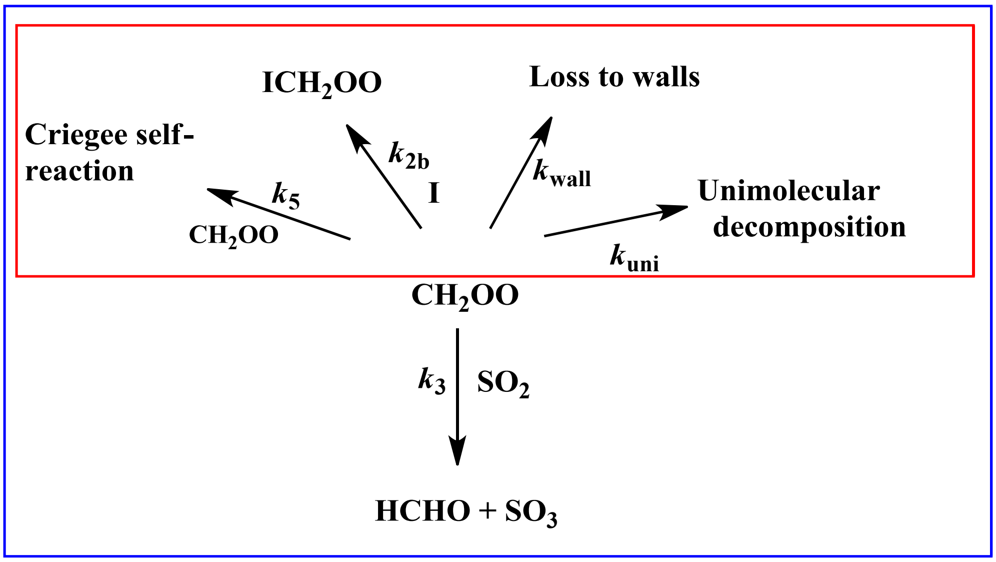

$$k'_{other}\ (s^{-1}) = \boxed{k_5[CH_2OO] + k_{wall} + k_{2b}[I] + k_{uni}}$$

$$k'_3\ (s^{-1}) = \boxed{k_3[SO_2] + k'_{other}}$$

The reactions in the red box have been lumped together as k_{other} and contain a mixture of first and second order processes. The sensitivity of the system has been improved in order to minimize the second-order radical-radical reactions such that if k_{other} (determined from CH_2OO decays in the absence of SO_2) is constrained to a first-order process then $k'_{other} < 250\ s^{-1}$. However, for this relatively low value of k'_{other}, the CH_2OO decays were mixed 1st and 2nd order (Figure S1) rather than the expected second order process if dominated by CH_2OO recombination (poor fit to second kinetics in the lowest panel of Fig S1), implying that the loss contribution from k_{wall} was still greater than self reaction or radical-radical reactions in these experiments. Fitting the mixed order decays indicates that the Criegee intermediate concentrations could conceivably have been below 1.0×10^{12} molecule cm^{-3}, however, a more conservative estimate of $[CH_2OO] = (1.5 \pm 0.5) \times 10^{12}$ molecule cm^{-3} is recommended.

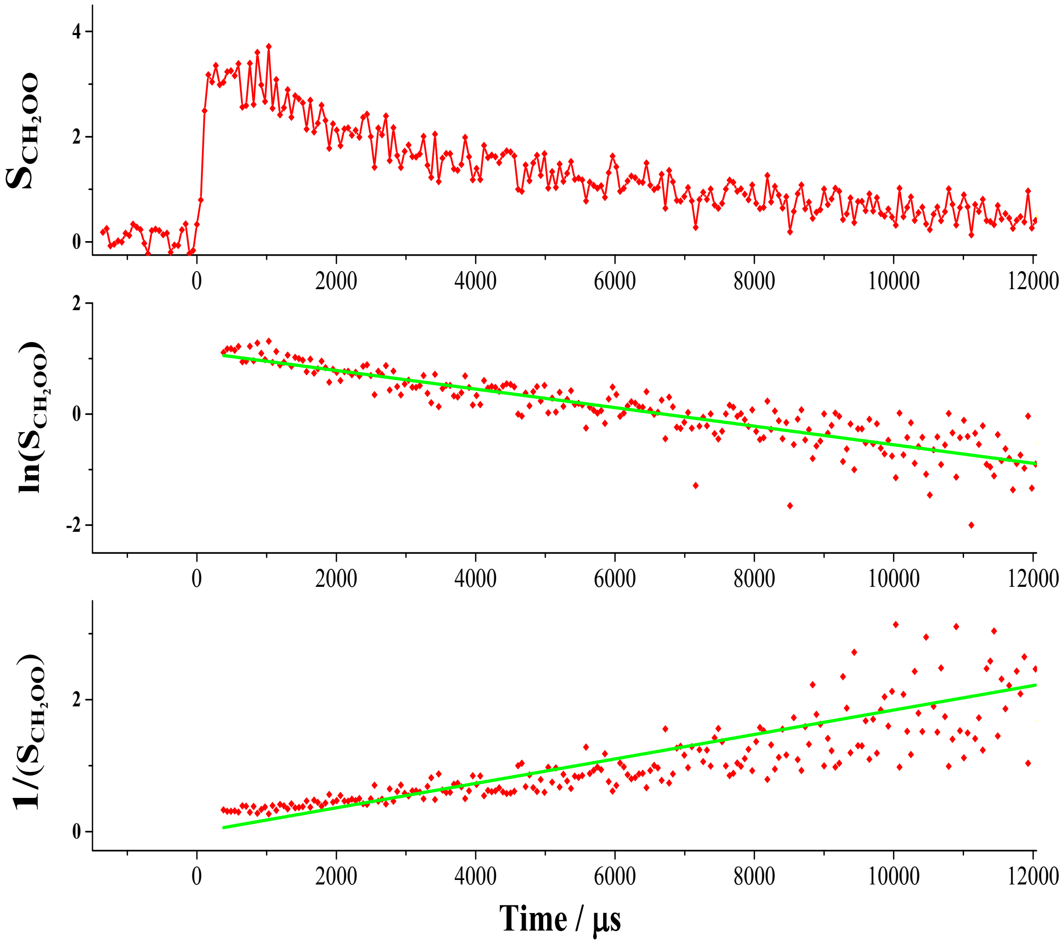

Fig. S1 The upper graph is a raw data set for CH_2OO decay in the absence of any SO_2. The middle graph is a first order plot of $\ln(S_{CH2OO})$ vs. time, here, the linear fit to the data is good, suggesting the decay trace still is more first order in nature than second order. The lower graph is a second order plot of $1/(S_{CH2OO})$ vs. time and the linear fit to the data is not very good, implying the second order characteristics are small. Note: S_{CH2OO} is equivalent to the observed experimental signal from CH_2OO.

Figure S2 shows a simulation of SO_2 and CH_2OO decays under conditions of low $[SO_2]$, 4.5 × 10^{12} molecule cm^{-3} and an initial CH_2OO concentration of 1.5 × 10^{12} molecule cm^{-3}. Although the ratio of the initial concentrations is only 3:1, wall loss is still a significant contribution to CH_2OO loss and therefore the concentration of $[SO_2]$ remains approximately constant. Pseudo-first-order concentrations are therefore maintained, see the traces in Figure S3, but at these very low concentrations of SO_2 the contribution of reaction 3 to CH_2OO removal is not dominant.

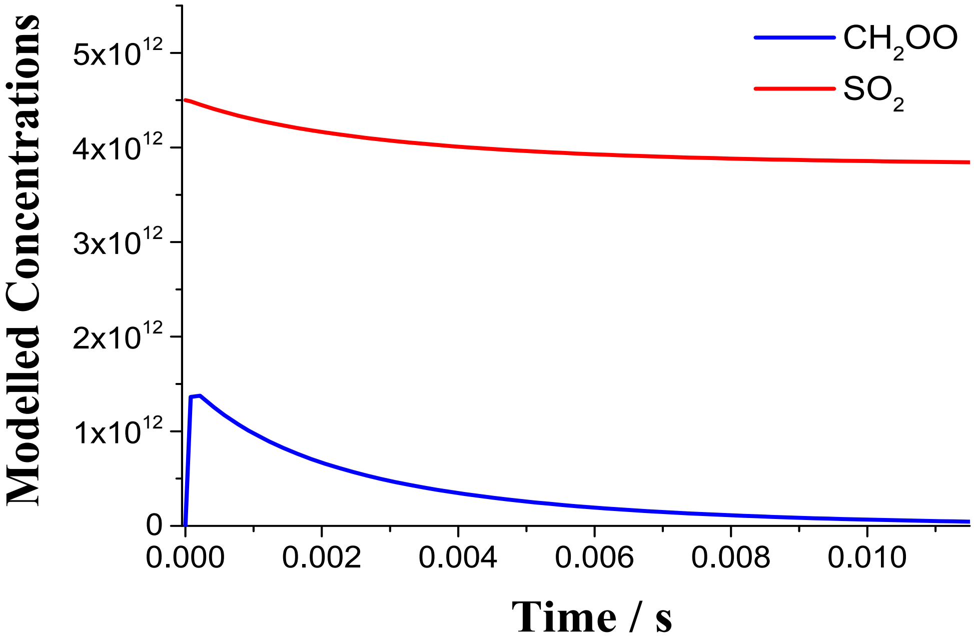

Fig. S2 A model of the $CH_2OO + SO_2$ reaction; $[CH_2OO] = 1.5 \times 10^{12}$ molecule cm^{-3}, $[SO_2] = 4.5 \times 10^{12}$ molecule cm^{-3}. An estimate of $k_{wall} = 100\ s^{-1}$ was used for modelling.

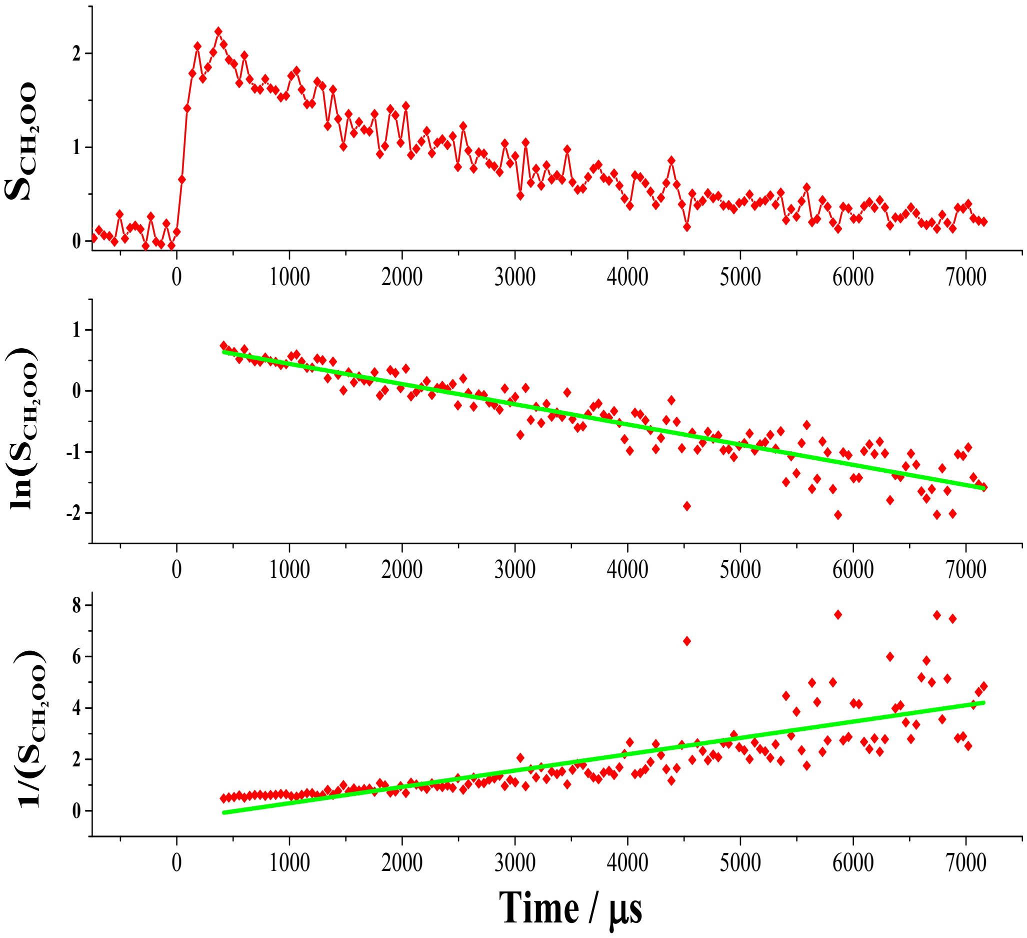

Fig. S3 The upper graph is a raw data set for CH_2OO decay with $[SO_2] \approx 4.5 \times 10^{12}$ molecule cm^{-3}. The middle graph is a first order plot of $\ln(S_{CH2OO})$ vs. time, here, the linear fit to the data is very good suggesting the system is more first order in nature than second. The lower graph is a second order plot of $1/(S_{CH2OO})$ vs. time and the linear fit to data is poor implying that the system is not second order. Note: S_{CH2OO} is equivalent to the experimental signal from CH_2OO observed.

2. Derivation of equations for fitting temporal profiles

If the flow rate of gas to and from the ionization region is equal, i.e. at steady-state, then the sampling can be described by Scheme 1:

$$\mathrm{R}_{\mathrm{reactor}} \xrightarrow{k_{\mathrm{sampling}}} \mathrm{R}_{\mathrm{ionization}}$$

Scheme 1. Transport of molecules from the reactor to the ionization region

Solving the kinetic equations describing Scheme 1 yields the temporal profile for molecules, R, in the reactor to reach the ionisation region, the sampling time, and is given by:

$$S_{detector,t} \propto R_{reactor,0}(1 - e^{-k_{eff}t}) \qquad \text{(E1)}$$

where $S_{\mathrm{detector},t}$ is the signal measured by mass spectrometer at time t (the photolysis laser is fired at $t = 0$) and is proportional to R_{reactor}, and $R_{\mathrm{reactor},0}$ is the concentration of the species in the reactor at time zero, and k_{eff} is the rate coefficient of the whole "sampling process".

If it is assumed that dilution in the sampling region is infinite – the dilution is reasonably expected to be large [1] - then there is no reaction in the sampling region, and the solution for this case is given by solving the differential equation where it is assumed that there is a steady-state between the reactor and the ionisation region:

$$\frac{d[CI]_{ionization}}{dt} + k_{eff}[CI]_{ionization} = k_{eff}[CI]_{reactor} \qquad \text{(E2)}$$

where $[\mathrm{CI}]_{\mathrm{ionization}}$ and $[\mathrm{CI}]_{\mathrm{reactor}}$ are the concentrations of Criegee Intermediate, CI, in the reactor and at the ionization region, respectively.

The kinetic equations governing the concentration of the CI in the reactor are:

$\mathrm{RI} + \mathrm{O_2} \rightarrow \mathrm{CI} + \mathrm{I}$ (R = $\mathrm{CH_2}$ or $\mathrm{CH_3CH}$) (R2)

$\mathrm{CI} + \mathrm{SO_2} \rightarrow$ Products (R3)

CI → loss (R4)

All reactions can be considered as first order or pseudo-first order with respect to CI and the rate coefficients for the two, parallel loss processes can be combined as k_3'.

$$\frac{d[CI]_{reactor,t}}{dt} = k_2^{'}[RI] - k_3^{'}[CI] \qquad \text{(E3)}$$

The concentration of RI as a function of time in the reactor is:

$$\frac{d[RI]}{dt} = k_2^{'}[RI] \qquad \text{(E4)}$$

Solution of E4 gives:

$$[RI]_t = [RI]_0 e^{-k_2^{'}t} \qquad \text{(E5)}$$

which can be substituted into E3. Solution of the resultant differential equation gives:

$$[CI]_{reactor,t} = \frac{RI_0 k_2^{'}}{k_2^{'} - k_3^{'}}[e^{k_3^{'}t} - e^{k_2^{'}t}] \qquad \text{(E6)}$$

This can be combined with E2 to give the final expression for the PIMS signal:

$$S_{CI,t} = \frac{P_1 k_2^{'} k_{eff}}{k_2^{'} - k_3^{'}}\left[\frac{e^{-k^{'}_2 \times t} - e^{-k_{eff} \times t}}{\left(k_{eff} - k^{'}_2\right)} - \frac{e^{-k^{'}_3 \times t} - e^{-k_{eff} \times t}}{\left(k_{eff} - k^{'}_3\right)}\right]$$

(E7)

where P_1 is the constant of proportionality linking the detector signal with the initial radical concentration.

3. Global Fitting of the $\mathrm{CH_2OO} + \mathrm{SO_2}$ data

Figure S4 shows examples of the global fits to the experimental decay traces at various concentrations of SO_2. For each trace there were number of global parameters (k_{eff}, k_2, k_3) and the local parameter $S_{C1height}$, the signal height which was varied for each trace. Concentrations of O_2 and SO_2 were local to each trace and determined the values of k_2' and k_3' for each experiment. The traces were weighted based on the reduced χ^2 value from the single trace analysis.

$$M_1 = \frac{(S_{C1height} \times k'_2 \times k_{eff})}{(k'_3 - k'_2)} \tag{E8}$$

$$M_2 = \frac{e^{-k'_2 \times t} - e^{-k_{eff} \times t}}{(k_{eff} - k'_2)} - \frac{e^{-k'_3 \times t} - e^{-k_{eff} \times t}}{(k_{eff} - k'_3)} \tag{E9}$$

$$S_{CH2OO} = M_1 \times M_2 + S_{bg} \tag{E10}$$

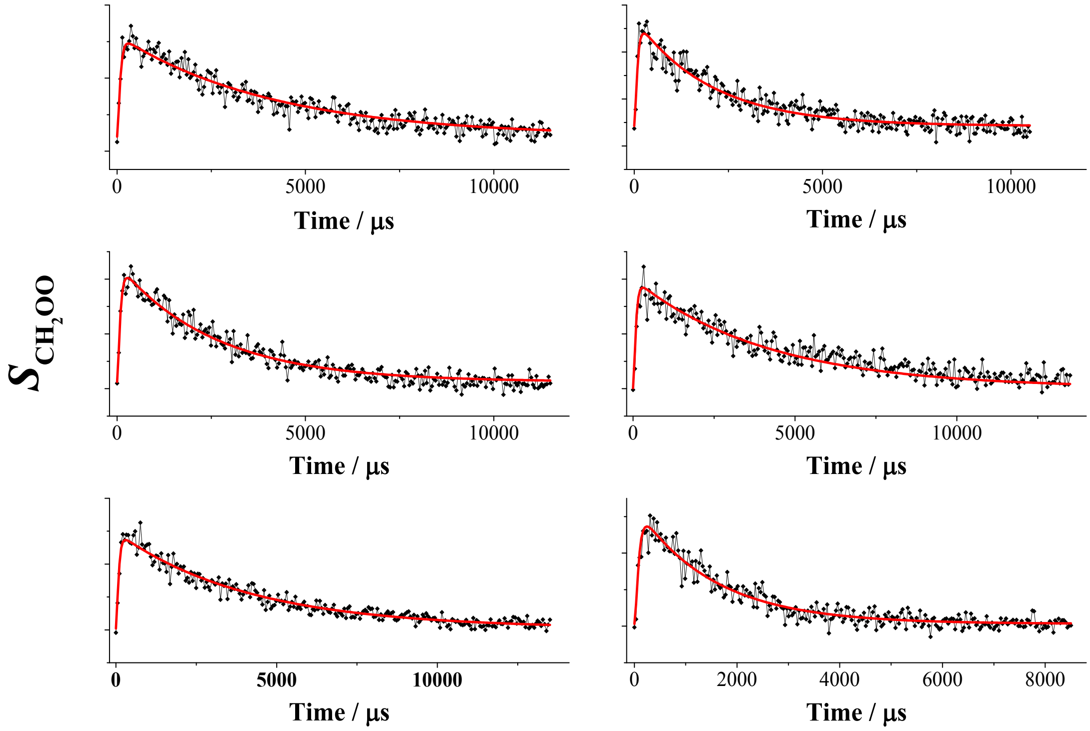

Fig. S4 An example of the global fitting which is plotted across several individual traces simultaneously; the fitting uses all of data to give the ‘global’ fit.

4. Simulations of the Chhantyal-Pun *et al.* data.

The reactions and the rate coefficients used to model the data are shown below (Table S1), and the initial conditions used in the model are listed in Table S2. Initially, the model was run in the absence of any SO_2 to see if it was possible to reproduce the data collected by Chhantyal-Pun *et al.*[2] This model was simple and excluded any ICH_2OO chemistry: ICH_2OO was assumed to be present in low concentrations due to the low pressures used (~7 Torr). Moreover, ICH_2OO is thought to react rapidly with CH_2OO ($k_{ICH2OO} \approx 2 \times 10^{-10}$ molecule^{-1} cm^{3} s^{-1}), therefore, if significant concentrations of ICH_2OO were present, the reaction between ICH_2OO and CH_2OO would have been the dominant loss process for CH_2OO. However, Chhantyal-Pun *et al.* suggest that 2nd order loss from the Criegee self-reaction is the dominant sink for CH_2OO. This means that any ICH_2OO formed is only present in small amounts.

Table S1 The simplified version of the model used to reproduce the data from Chhantyal-Pun *et al.* All the rate coefficients listed are from Chhantyal-Pun *et al.*, except k_2, which is an IUPAC recommended value for $p \approx 7$ Torr.

Reaction	Rate coefficient
$CH_2I + O_2 \rightarrow CH_2OO + I$	$k_2 = 1.5 \times 10^{-12}$ molecule^{-1} cm^{3} s^{-1}
$CH_2OO + CH_2OO \rightarrow 2\ HCHO + O_2$	$k_{C1SR} = 7.35 \times 10^{-11}$ molecule^{-1} cm^{3} s^{-1}
$CH_2OO + I \rightarrow$ products	$k_{C1+I} = 1 \times 10^{-11}$ molecule^{-1} cm^{3} s^{-1}
$CH_2OO + SO_2 \rightarrow$ products	$k_3 = 7.46 \times 10^{-11}$ molecule^{-1} cm^{3} s^{-1} or $k_3 = 3.80 \times 10^{-11}$ molecule^{-1} cm^{3} s^{-1}
$CH_2OO \rightarrow$ products	$k_{uni} = 11.6$ s^{-1}

Table S2 Initial concentrations of reactants used in the Kintecus model.[3]

Species	**Initial concentration / molecule cm^{-3}**
CH_2I	5.0×10^{12}
O_2	3.0×10^{16}
I	5.0×10^{12}
CH_2OO	0
SO_2	Variable

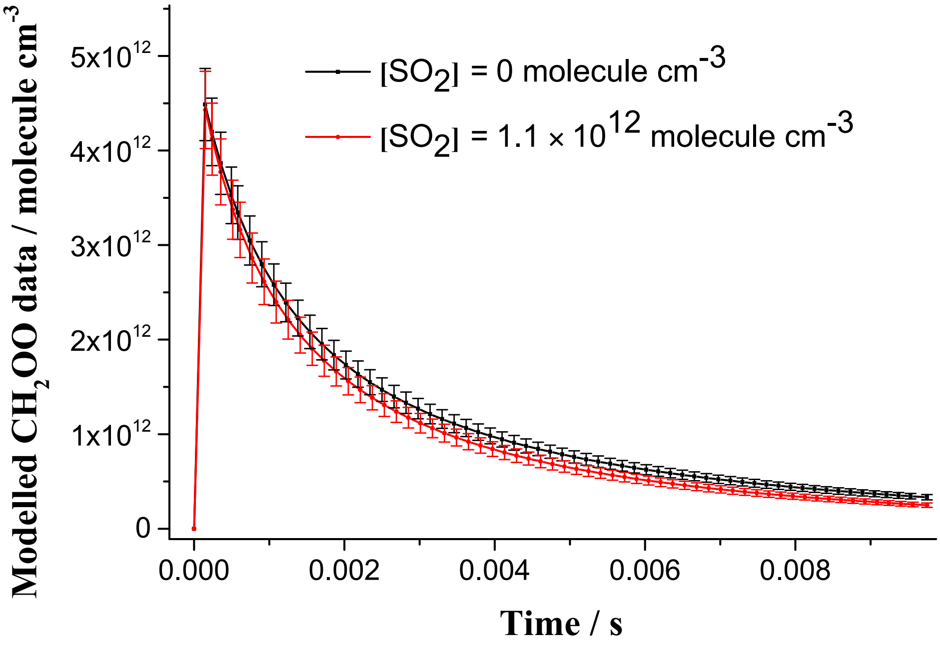

Fig. S5 A comparison of the simulated CH_2OO decay when [SO_2] = 0 molecule cm^{-3} and when [SO_2] = 1.1 × 10^{12} molecule cm^{-3}. The error quoted for the model run with SO_2 in the system is 9 %, this was calculated by propagating the errors associate with k_{C1SR} and k_3.

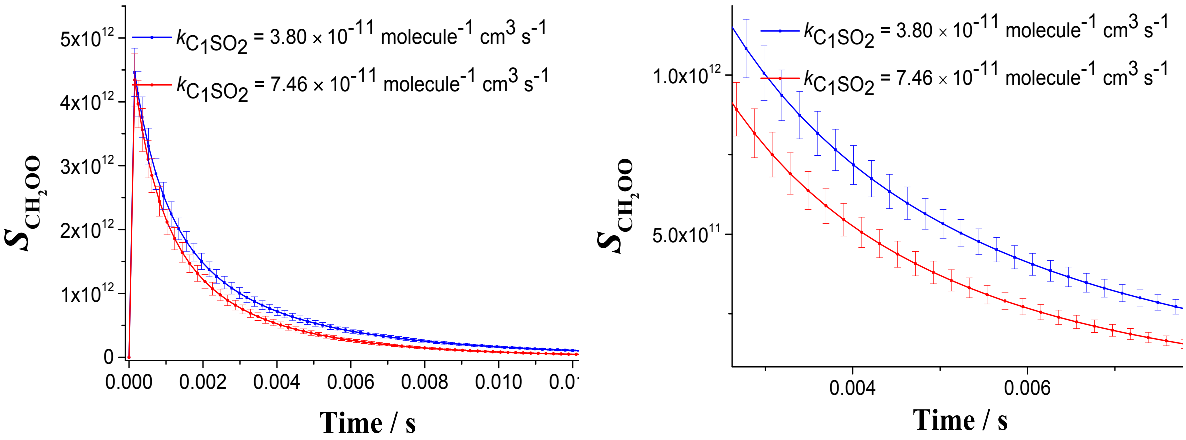

Fig. S6 (a) A comparison of the reaction system when [SO_2] = 5 × 10^{12} molecule cm^{-3}; Note that k_3 = 3.80 × 10^{-11} molecule^{-1} cm^3 s^{-1} (blue) and k_3 = 7.46 × 10^{-11} molecule^{-1} cm^3 s^{-1} (red); (b) The expanded scale highlights that the datasets are significantly different from each other. The error bars quoted for the model with SO_2 is ~9.5 % for k_3 = 7.46 × 10^{-11} molecule^{-1} cm^3 s^{-1} and ~8.5 % for k_3 = 3.80 × 10^{-11} molecule^{-1} cm^3 s^{-1}, this was calculated by propagating the errors associated with k_{C1SR} and k_3.

Simulations of the data of Chhantyal-Pun *et al.* (Fig S5) shows that the [CH_2OO] changes by less than 7% at ~ $t_{1/2}$ (~1.1 ms) for the addition of 1 × 10^{12} SO_2 over the baseline case of zero added SO_2, and only exceeds 15% after ~5 ms where over 80% of the initial CH_2OO has been consumed and where secondary chemistry may play more of a role. At $[SO_2] = 5 \times 10^{12}$, we have simulated the CH_2OO decay for $k_3 = 3.80$ and 7.46×10^{-11} cm^3 molecule^{-1} s^{-1} as shown in Fig. S6. At $t_{1/2}$ for the slower decay, 0.93 ms, the $[CH_2OO]$ with the higher k_3 rate coefficient is only 10% lower. Note how the $t_{1/2}$ value of the simulated data of Chhantyl-Pun *et al.* contrasts with our TRUVAS data at similar $[SO_2]$ where $t_{1/2}$ is ~3 ms; whatever the value of k_3, the decays in the Chhantyl-Pun *et al.* studies are dominated by reactions other than R3. At 4 ms, corresponding to >80% removal of $[CH_2OO]_0$ with the lower rate coefficient, the simulated $[CH_2OO]$ is 20% lower, however, this is again in the tail of the decay (see Fig S6(b)). The simulations show that the contribution of reaction 3 to the CH_2OO decays at low $[SO_2]$ is quite small and therefore that differences between the higher and lower values reported by Chhantyal-Pun *et al.* are also small. The precision of the data reported by Chhantyal-Pun *et al.* is such, that these differences can be reproducibly extracted from the experimental decays which are dominated by recombination kinetics, however, it is possible that other explanations, such as secondary chemistry, may account for these differences.

5. Details on the global fitting of CH_3CHOO and CH_3CHO data

It was observed that there is both small instant signal and a slow secondary growth at *m/z* = 44; it was therefore decided that a global fitting should be used, this time fitting both the CH_3CHOO decays and the species formed at *m/z* = 44 simultaneously. To fit both data-sets the equations previously used required significant adaptation, including the addition of a second ‘z’ parameter (z1) within the spreadsheet and an if-statement to allow the correct function to be selected for the CH_3CHOO and CH_3CHO data respectively (E S1-S10):

If $z1 = 1$:

$$M_1 = \frac{(S_{C2height} \times k'_9 \times k_{eff})}{(k'_{C1total} - k'_9)} \tag{E S1}$$

$$M_2 = \frac{e^{-k'_9 \times t} - e^{-k_{eff} \times t}}{(k_{eff} - k'_9)} - \frac{e^{-k'_{10} \times t} - e^{-k_{eff} \times t}}{(k_{eff} - k'_{10})} \tag{E S2}$$

$$S_{CH3CHOO} = M_1 \times M_2 + S_{bg} \tag{E S3}$$

$$k'_{10,\ CH3CHOO} = (k_{10} \times [SO_2]) + k_{wall} + k_X \tag{E S4}$$

If $z1 = 2$:

$$Y_{CH3CHO} = S_{CH3CHOheight} \times A \times \left(\frac{(k_{10} \times [SO_2]) + k_X}{k'_{10,CH3CHO}}\right) \tag{E S5}$$

$$N_1 = \frac{(Y_{CH3CHO} \times k'_{CH3CHO} \times k_{eff})}{(k'_{LossCH3CHO} - k'_{10,CH3CHO})} \tag{E S6}$$

$$N_2 = \frac{e^{-k'_{10,CH3CHO} \times t} - e^{-k_{eff} \times t}}{(k_{eff} - k'_{10,CH3CHO})} - \frac{e^{-k'_{2ndryCH3CHO} \times t} - e^{-k_{eff} \times t}}{(k_{eff} - k'_{LossCH3CHO})} \tag{E S7}$$

$$N_3 = \frac{(S_{instant} \times k_{eff})}{(k_{eff} - k'_{LossCH3CHO})} \times \left(e^{-k_{2ndryCH3CHO} \times t} - e^{-k_{eff} \times t}\right) \tag{E S8}$$

$$S_{CH3CHO} = N_1 \times N_2 + N_3 + S_{bg2} \tag{E S9}$$

$$k'_{10,CH3CHO} = (k_{10} \times [SO_2]) + k_{wall} + k_X \tag{E S10}$$

A number of new parameters have been introduced in E S1-10: k'_{CH3CHO} is the rate coefficient of the acetaldehyde formation; k_X is the rate coefficient of other reactions which contribute to the production of CH_3CHO (e.g. I atom chemistry), excluding the wall losses (k_{wall}); Y_{CH3CHO} is equivalent to the yield of acetaldehyde formed; $S_{CH3CHOheight}$ represents the maximum height of the CH_3CHO signal; A is a scaling factor; $k_{LossCH3CHO}$ is equivalent to loss rate of acetaldehyde; $S_{instant}$ is equal to the signal height of any instant CH_3CHO observed; and S_{bg2} represented the background signal at $m/z = 44$.

Using the equations listed above it was possible to fit the whole data-set at once, and as many of the parameters as possible were shared in the analysis: k_{C1SO2}, k_X, k_{wall}, $k_{CH2I+O2}$, k_{eff}, $k_{2ndaryCH3CHO}$, $S_{instant}$. Some of the parameters were kept constant (k_{eff}, S_{bg} and S_{bg2}) and the rest were allowed to float during the iterations of the fitting until χ^2 was minimised. Using this technique a rate coefficient of $k_{10} = (1.3\pm0.3) \times 10^{-11}$ molecule^{-1} cm^3 s^{-1} was evaluated. A significant error is associated with this evaluation as k_{10} was very sensitive to $S_{instant}$; the precise value of $S_{instant}$ was unknown, although it could be estimated from the traces where $[SO_2] = 0$ molecule cm^{-3}. That being said, the rate coefficient determined using this methodology is in agreement with both the earlier work from this study and with literature values.[4]

As mentioned above, it was apparent that there was another channel augmenting the signal at $m/z = 44$. To determine if any acetaldehyde was produced from $CH_3CHOO + SO_2$, alternative equations were used in the global analysis for both the rate of acetaldehyde formation and the yield of acetaldehyde (E S11-12). Notably, these equations suggest that acetaldehyde formation is entirely independent of the $CH_3CHOO + SO_2$ reaction.

$$k'_{CH3CHO} = k_{wall} + k_X \tag{E S11}$$

$$Y_{CH3CHO} = S_{CH3CHOheight} \times A \times \left(\frac{k_X}{k'_{CH3CHO}}\right) \tag{E S12}$$

When using equations S11-12 to fit the data it was apparent that these equations could not produce a good fit to the data (Figure S7 (Right)). As the better fit to the data is yielded from the full model (Fig S7 (Left)), it suggests the acetaldehyde signal is dependent on the CH_3CHOO + SO_2 reaction. Therefore, this reaction must be partially responsible for the signal at $m/z = 44$, proving that these species correlated with each other.

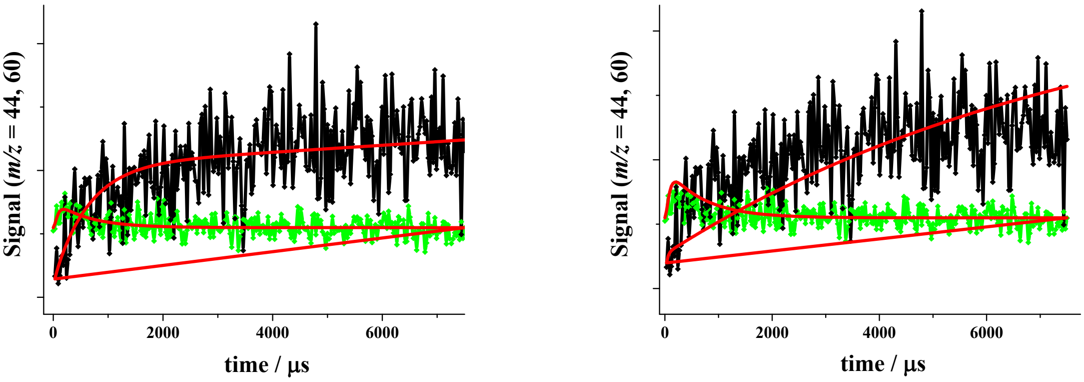

Fig. S7 :(Left) A plot of the data fitted using the Criegee dependent equations (E S1-10); (Right) A plot of the same data, here the Criegee independent equations were used to fit the data (E S10-11). The green points are the Criegee data and the black points acetaldehyde. The red fit is the global fit to both species.

It should be noted that other possible products from the reaction were searched for, although none were found. This is not entirely surprising as the ionization potential of SO_3 is thought to be ~13 eV [5]. There was also no sign of the secondary ozonide at $m/z = 124$, this was very close to the I atom signal at $m/z = 127$ (a very large and broad peak); it is therefore plausible that signal from the SOZ may have been masked by this signal. It is also possible that any SOZ formed was fragmented by the photoionization beam. In fact it is possible that the acetaldehyde observed is actually produced during photoionization rather than by unimolecular decomposition. That said, as all of the experiments were conducted at low pressures ($p < 2.5$ Torr) it is thought that unimolecular decomposition channel will be dominant under these condition. For future work, experiments could be conducted to test whether the CH_3CHO formed is from photoionization or decomposition; during these experiments a scavenger for CH_3CHO would be added to the system (such as chlorine radicals). If the CH_3CHO was formed by unimolecular decomposition, the CH_3CHO would react with the scavenger and the signal at $m/z = 44$ would be depleted. However, if the CH_3CHO was formed during photoionization, there would be insufficient time any scavenging to occur and signal at $m/z = 44$ would persist.

6. Atmospheric Implications

In polluted environments such as mega cities it is plausible that the C_2 + SO_2 reaction may be responsible for > 1 % of the *syn*-CH_3CHOO destruction. For example, in Beijing, China an average concentration of SO_2 of $[SO_2] > 2.5 \times 10^{11}$ molecule cm^{-3} was recorded.[6] Under these conditions it is plausible that the reaction with SO_2 may be responsible for ~5 % of the *syn*-

CH_3CHOO loss. This model may well be a slight over-estimate of the importance of this channel, as the kinetics of other minor destruction channels (primarily the carboxylic acids) were not taken into account. That being said, these results do suggest that in certain environments SO_2 may play a significant role in C_2 Criegee destruction. In terms of SO_2 oxidation, this process will be of particular importance at night when OH concentrations are low (OH + SO_2 is the dominant oxidation process).

Table S3: Major loss channels for the C_2 CI

Temp. / K	**Environment**	**RH / %**	**$[H_2O]$ / cm^{-3}**	**$[(H_2O)_2]$ / cm^{-3}**	**$[SO_2]$ / cm^{-3}**	**% loss H_2O**	**% loss $(H_2O)_2$**	**% loss SO_2**
298	Mega City	75	5.8×10^{17}	5.5×10^{14}	2.5×10^{11}	2.6	97.0	0.4
298	Mega City	50	3.9×10^{17}	2.4×10^{14}	2.5×10^{11}	3.8	95.2	0.9
298	Rural Area	75	5.8×10^{17}	5.5×10^{14}	2.0×10^{10}	2.6	97.4	0.0
298	Rural Area	50	3.9×10^{17}	2.4×10^{14}	2.0×10^{10}	3.9	96.1	0.1
283	Mega City	75	2.3×10^{17}	9.9×10^{13}	2.5×10^{11}	6.1	91.4	2.5
283	Mega City	50	1.6×10^{17}	4.4×10^{13}	2.5×10^{11}	8.6	86.2	5.2
283	Rural Area	75	2.3×10^{17}	$9.\ \times10^{13}$	2.0×10^{10}	6.2	93.6	0.2
283	Rural Area	50	1.6×10^{17}	4.4×10^{13}	2.0×10^{10}	9.0	90.5	0.4

6. References

1. R. W. Carr, *Adv. Photochem. FIELD Full Journal Title:Advances in Photochemistry*, 1999, **25**, 1-57.
2. R. Chhantyal-Pun, A. Davey, D. E. Shallcross, C. J. Percival and A. J. Orr-Ewing, *Phys. Chem. Chem. Phys.*, 2015, **17**, 3617-3626.
3. J. C. Ianni, *Kintecus, Windows Version 2.80, www.kintecus.com*, www.kintecus.com.
4. M. C. Smith, C. H. Chang, W. Chao, L. C. Lin, K. Takahashi, K. A. Boering and J. J. M. Lin, *J. Phys. Chem. Lett.*, 2015, **6**, 2708-2713.
5. K. B. Snow and T. F. Thomas, *International journal of mass spectrometry and ion processes*, 1990, **96**, 49-68.
6. W. Lin, X. Xu, Z. Ma, H. Zhao, X. Liu and Y. Wang, *Journal of Environmental Sciences*, 2012, **24**, 34-49.